Atmos. Chem. Phys. Discuss., 13, 3575–3611, 2013
www.atmos-chem-phys-discuss.net/13/3575/2013/
doi:10.5194/acpd-13-3575-2013

Atmospheric Chemistry and Physics
Open Access
Discussions

This discussion paper is/has been under review for the journal Atmospheric Chemistry and Physics (ACP). Please refer to the corresponding final paper in ACP if available.

Cloud-resolving simulations of mercury scavenging and deposition in thunderstorms

U. S. Nair[1], Y. Wu[2], C. D. Holmes[3], A. Ter Schure[4], G. Kallos[5], and J. T. Walters[6]

[1]Department of Atmospheric Science, University of Alabama in Huntsville, 320 Sparkman Drive, Alabama 35805, USA
[2]Earth System Science Center, University of Alabama in Huntsville, 320 Sparkman Drive, Huntsville, Alabama 35805, USA
[3]Department of Earth System Science, University of California, Irvine, California 92697, USA
[4]Electric Power Research Institute, Palo Alto, CA 94304, USA
[5]School of Physics, University of Athens, Athens, Greece
[6]Southern Company Services, Birmingham, AL 35203, USA

Received: 26 November 2012 – Accepted: 14 January 2013 – Published: 8 February 2013

Correspondence to: Y. Wu (wuy@nsstc.uah.edu)

Published by Copernicus Publications on behalf of the European Geosciences Union.

Abstract

This study examines dynamical and microphysical features of convective clouds that affect mercury (Hg) wet scavenging and concentrations in rainfall. Using idealized numerical model simulations in the Regional Atmospheric Modeling System (RAMS), we diagnose vertical transport and scavenging of soluble Hg species in thunderstorms under typical environmental conditions found in the Northeast and Southeast United States (US). Three important environmental characteristics that impact thunderstorm morphology were studied: convective available potential energy (CAPE), vertical shear (0–6 km) of horizontal wind (SHEAR) and precipitable water (PW).

We find that in a strong convective storm in the Southeast US that about 40 % of mercury in the boundary layer (0–2 km) can be scavenged and deposited to the surface. Removal efficiencies are 35 % or less in the free troposphere and decline with altitude. Nevertheless, if we assume that soluble Hg species are initially uniformly mixed vertically, then about 60 % deposited mercury deposited by the thunderstorm originates in the free troposphere.

For a given CAPE, storm morphology and Hg deposition respond to SHEAR and PW. Experiments show that the response of mercury concentration in rainfall to SHEAR depends on the amount of PW. For low PW, increasing SHEAR decreases mercury concentrations in high-rain amounts (> 13 mm). However, at higher PW values, increasing SHEAR decreases mercury concentrations for all rainfall amounts. These experiments suggest that variations in environmental characteristics relevant to thunderstorm formation and evolution can also contribute to geographical difference in wet deposition of mercury.

An ensemble of thunderstorm simulations was also conducted for different combinations of CAPE, SHEAR and PW values derived from radiosonde observations at five sites in the Northeast United States (US) and at three sites in the Southeast US. Using identical initial concentrations of gaseous oxidized mercury (GOM) and particle-bound mercury (HgP), from the GEOS-Chem model, the simulations predict higher mercury

ACPD

13, 3575–3611, 2013

concentrations in rainfall from thunderstorms forming in the environmental conditions over the Southeast US compared to the Northeast US.

Mercury concentrations in rainfall are also simulated for a typical stratiform rain event and found to be less than in thunderstorms forming in environments typical of the Southeast US. The stratiform cloud scavenges mercury from the lower ∼ 4 km of the atmosphere, while thunderstorms scavenge up to ∼ 10 km.

1 Introduction

Lakes, rivers and coastal waters throughout the United States contain mercury at levels that harm wildlife and people who consume fish from these waters (EPA, 2011). Monitoring has established that atmospheric transport and deposition is a major source of mercury to many of these watersheds (Lindberg et al., 2007; Northeast Regional Mercury Total Maximum Daily Load, 2007). In the Eastern United States, wet deposition is largest over the Gulf Coast region (Fig. 1), particularly during the summer months, coinciding with the peak of convective storm activity. Indeed, rainwater samples from thunderstorms contain higher mercury concentrations than rain from non-convective or weakly convective storms (Holmes et al., 2010b).

The causes of enhanced mercury concentrations in thunderstorm rain remain unclear. The enhancement might be due to the large volumes of boundary layer air that are sucked into the convective updraft, where scavenging can occur (Dvonch et al., 1998, 2005; White et al., 2009). Alternatively, deep convective thunderstorms may scavenge from a high-altitude reservoir of soluble mercury that is inaccessible to weak or non-convective storms (Guentzel et al., 2001; Selin and Jacob, 2008; Landing et al., 2010). Soluble mercury species consist of gaseous oxidized mercury (GOM) and particle-bound mercury (HgP), both of which can be scavenged by cloud water and precipitation. These species are emitted directly from coal-fired power plants and some other industrial sources and can also be produced by oxidation of elemental mercury (Hg(0)), the dominant form of atmospheric mercury. The Eastern US has large mercury

ACPD
13, 3575–3611, 2013

emissions and aircraft have documented the increase of oxidized mercury with altitude (Sillman et al., 2007; Talbot et al., 2007; Lyman and Jaffe, 2012), so both mechanisms may plausibly influence mercury concentrations in thunderstorms. The interplay and importance of these mechanisms, however, depends on the dynamics of thunderstorms and their atmospheric environment.

Prior studies have examined the role of cloud dynamics and microphysics on the transport and scavenging of atmospheric trace species (Cotton et al., 1995; Cohen, 2000; Yin et al., 2001; Barth et al., 2007; Halland et al., 2009). Cotton et al. (1995) found that cloud venting, or transport of boundary layer air by storms to upper levels, varies substantially as a function of storm type (Cotton et al., 1995), with the extratropical cyclones being most efficient followed by mesoscale convective systems (excluding mesoscale convective complex's), ordinary thunderstorms, tropical cyclones and convective complexes. Environmental characteristics, such as atmospheric instability, impact the mixing of air from surroundings into the thunderstorms (Cohen, 2000). Thunderstorms that form in maritime environments better scavenge soluble trace gases from the atmosphere compared to those that form in a continental setting (Yin et al., 2001), even after accounting for differences in amount of total rainfall between these two settings. Prior studies also show the viability of utilizing cloud-resolving models in understating processes related to removal and transport of trace species by convective storms (Barth et al., 2007; Halland et al., 2009).

This study uses cloud-resolving simulations of convective and non-convective rainstorms to examine mercury transport within clouds, including its scavenging by precipitation and deposition to the ground. We also test how ambient atmospheric conditions affect scavenging, based on the well-known ways that these properties affect thunderstorm dynamics, morphology and microphysics (e.g. Cotton et al., 1995). Through analysis of radiosonde data, we identify atmospheric conditions – specifically, convective available potential energy (CAPE), shear and precipitable water – that differ between the Northeast and Southeast United States. With simulations of thunderstorms occurring under each of these regions, and assuming the same initial distribution of GOM

ACPD
13, 3575–3611, 2013

and HgP, we show that meteorological controls on cloud dynamics and microphysics likely explain part of the regional enhancement of mercury deposition in the Southeast.

2 Methods

2.1 Meteorological data

Three important factors that potentially modulate mercury wet deposition in thunderstorms are the nature of the updraft, vertical variation of horizontal wind in the environment and hydrometeor mixing ratio within clouds. A substantial amount of the air within thunderstorms originates from within the PBL (Dickerson et al., 1987; Cotton et al., 1995). Thus the mass flux and the incorporation of PBL air in thunderstorm are influenced by the updraft vertical velocity. Small-scale turbulent and larger-scale cloud entrainment also incorporates free tropospheric air into thunderstorms (Knupp and Cotton, 1985). Further, there are two forms of small-scale turbulent entrainment: lateral and cloud top entrainment. Of these, cloud top entrainment is more effective and is driven by fluid shear instabilities that engulf environmental air along the cloud edge caused by horizontal variations in updraft strength. Subsequent evaporation of cloud within engulfed air leads to downdrafts that penetrate and mix environmental air over depths of 1–2 km (Knupp and Cotton, 1985). Larger-scale systematic lateral entrainment, under conditions without environmental shear, occurs due to increasing vertical velocity with height and associated lateral flow driven by mass continuity requirements. In sheared environments, high pressure perturbation on the upshear side of thunderstorms diverts the environmental flow and causes a relatively unmixed cloud region. However, an associated low pressure perturbation feature on the down shear side causes flow reversal and wake entrainment, mixing environmental air into thunderstorms. Unlike turbulent entrainment, wake entrainment is organized at cloud scale. In addition, the magnitude of pressure perturbations that drive wake entrainment flow is proportional to vertical shear of horizontal wind and also the gradient of vertical velocity. Knupp and Cotton

ACPD
13, 3575–3611, 2013

(1995) notes that the relative strengths of the turbulent scale and large-scale entrainment are potentially modulated by environmental characteristics, with the large-scale entrainment becoming more dominant as the storm vigor increase. Numerical modeling studies of Cohen (2000) do indeed show such modulation of cloud entrainment processes, with stronger updrafts in unstable environments being able better entrain undisturbed environmental air compared to weak updrafts in more stable environment.

In the context of the physical process settings discussed above, the experimental design utilized in this study focuses on thunderstorm morphology and evolution based on a parameter space defined by three variables, namely Convective Available Potential Energy (referred from hereon as CAPE), vertical shear (vertical component of gradient) of horizontal wind (referred from hereon as SHEAR) and precipitable water (referred from hereon as PW). Note that CAPE is the potential energy that is available to a parcel ascending from the level of free convection to the equilibrium level. CAPE is indicative of the atmospheric instability and value ranges of less than 1000 $\mathrm{J\,kg^{-1}}$, 1000–2500 $\mathrm{J\,kg^{-1}}$ and greater than 2500 $\mathrm{J\,kg^{-1}}$ are considered weakly unstable, moderately unstable and largely unstable respectively. CAPE is also indicative of the maximum updraft speed since it the amount of energy available for conversion to kinetic energy. As discussed previously, higher SHEAR leads to better organized flows, especially those related to larger-scale entrainment. PW is the total amount of water vapor available within an atmospheric column and is expressed as the height (usually in mm) of the column of liquid water obtained from condensing all the water vapor within an atmospheric column of cross section 1 $\mathrm{m^2}$. PW impacts the amount of condensate present within the updraft and thus the vertical velocity. The three parameter space used in this study is a subset of higher dimensional parameter spaces utilized by prior numerical modeling studies of thunderstorm morphology and evolution (Cohen, 2000; McCaul and Weissman, 2001; McCaul et al., 2005; Cohen and McCaul, 2006; Kirkpatrick et al., 2007; Kirkpatrick et al., 2011). Note that these studies do show that CAPE, SHEAR and PW modulate cloud mass flux, cloud entrainment and hydrometeor mass distribution

Discussion Paper | Discussion Paper | Discussion Paper | Discussion Paper |

ACPD
13, 3575–3611, 2013

Title Page
Abstract | Introduction
Conclusions | References
Tables | Figures
◀| |▶
◀ ▶
Back | Close
Full Screen / Esc
Printer-friendly Version
Interactive Discussion

in thunderstorms and all of these processes are important to wet deposition removal of atmospheric mercury.

The three-parameter space utilized in this study is defined by discrete ranges of CAPE, SHEAR and PW (Table 1). The ranges represent different possible combinations of these parameters. Occurrences of these parameter combinations are determined by analyzing radiosonde observations from five Northeast sites (∼ 40° N) and three Southeast sites (∼ 30° N) for the summer months 2001–2011 (Fig. 2) using the methodology of Nair et al. (2002).

2.2 Model description

The Reginal Atmospheric Modeling System (RAMS) is a non-hydrostatic finite difference numerical model used to simulate atmospheric phenomena ranging from cloud scale to mesoscale (Cotton et al., 2003). In this study, the RAMS version 6.0 is configured to simulate individual thunderstorms, their internal convective motions and resultant precipitation. Similar to McCaul et al. (2005), we use an idealized experimental design to highlight the role of environmental conditions on storm morphology and mercury. The horizontal domain consists of flat terrain extending 120 km × 120 km with a spacing of 500 m in each dimension. The vertical resolution is 20 m near the ground, increasing to 1000 m at high altitudes, up to model top at 23.5 km. Cyclic lateral boundary conditions are used.

Two soluble mercury species, GOM and HgP, are included in the simulations here. These species are transported by bulk air motions and within precipitation. Exchange of GOM and HgP between air, cloud water and precipitation follow a scheme for nitric acid and inert aerosols (Seinfeld and Pandis, 2006) as implemented in RAMS by Voudouri and Kallos (2007). Within clouds, GOM concentrations in cloud water are in Henry's law equilibrium with the interstitial air, while HgP is assumed to reside entirely in the condensed water or ice. The dissolved fractions of GOM and HgP are then transported downward by hydrometeors at the same rate that precipitation forms. Below clouds, GOM is scavenged by rain following the Levine and Schwartz (1982) mechanism for

Discussion Paper | Discussion Paper | Discussion Paper | Discussion Paper |

ACPD
13, 3575–3611, 2013

Simulations of mercury scavenging and deposition in thunderstorms

U. S. Nair et al.

Title Page
Abstract Introduction
Conclusions References
Tables Figures
◀| |▶
◀ ▶
Back Close
Full Screen / Esc
Printer-friendly Version
Interactive Discussion

nitric acid (see also Eq. 20.25 of Seinfeld and Pandis, 2006). Falling rain and ice scavenge HgP with collision efficiencies calculated for monodisperse aerosols with diameter 300 nm (see Eq. 20.53 of Seinfeld and Pandis, 2006). Both GOM and HgP are released back to the air if hydrometeors evaporate before reaching the ground. Ice is assumed not to scavenge GOM (Sigler et al., 2009; Amos et al., 2012), so no GOM is scavenged below −39 °C. This wet deposition scheme has been evaluated against observations from the Mercury Deposition Network (MDN) in the Eastern United States. During periods when RAMS accurately simulates precipitation amounts, the model reproduces about half of the observed variability in mercury deposition, similar to the CMAQ-Hg model (Voudouri and Kallos, 2007).

The model is initialized with horizontally uniform vertical profiles of wind and thermodynamic variables. A warm air bubble is inserted at the surface to trigger convection and its subsequent evolution is simulated for 2 h. Over these short time scales, atmospheric radiative transfer and land-atmosphere interactions have little effect on storm development and are neglected here. We use a detailed cloud microphysical parameterization, with prognostic equations for mixing ratios of cloud water, rain, pristine ice, snow, aggregate, graupel and hail hydrometeors (Walko et al., 1995; Meyers et al., 1997).

2.3 Initial vertical Hg profiles

Initial conditions for GOM and HgP (Fig. 3) are for summer conditions over the Southeast US, as simulated by GEOS-Chem global Hg model (Holmes et al., 2010a) since vertically resolved observations of GOM and HgP are rare. The global model includes oxidation of Hg(0) by bromine and Coburn et al. (2011) have recently observed BrO in the marine boundary layer and free troposphere near our study area. The initial conditions include surface concentrations of GOM around 10 pg m^{-3}, which is similar to suburban and rural observations in the Southeast US (Edgerton et al., 2006; Valente et al., 2007). The GEOS-Chem model also reproduces observed vertical gradients of Hg(0), including in the lower stratosphere at mid-latitudes (Holmes et al., 2010a). Simulated

ACPD
13, 3575–3611, 2013

GOM and HgP concentrations near the tropopause are smaller than reported by Lyman and Jaffe (2012) ($120\,\mathrm{pg\,m^{-3}}$ vs. $500\,\mathrm{pg\,m^{-3}}$ for total oxidized Hg at 15 km) but show a similarly sharply increasing vertical gradient in the lower stratosphere. At higher altitudes, Lyman and Jaffe (2012) suggest that there is little Hg of any kind above 17 km, due to aerosol scavenging and gravitational sedimentation. These aerosol processes are not included in the GEOS-Chem model, but the results of this work are not sensitive to this assumption because, as shown below, there is little wet scavenging from these stratospheric altitudes. In the present study, equal amounts of GOM and HgP are assumed for simplicity so that all differences in scavenging and deposition of these species are due to interactions with hydrometeors. Select simulations using uniform GOM and HgP initial conditions are described further below.

2.4 Numerical modeling experiments

Three types of experiments are conducted: (1) diagnosis of how a typical thunderstorm transports mercury vertically through advection and precipitation, including surface deposition (2) simulations of thunderstorms that form and evolve in environments with differing combinations of CAPE, SHEAR and PW and associated sensitivity experiments to isolate the effect of SHEAR and; (3) simulation of a stratiform rainfall event to compare the efficacy of removal of mercury between deep convective and stratiform systems. The first experimental case study traces the fate of mercury, including wet deposition, during a strong thunderstorm that occurs under conditions in the Southeast US (c2500s10p60_s). Six simulations are run with $30\,\mathrm{pg\,m^{-3}}$ of GOM and HgP initially spread uniformly over the following altitude ranges: the entire depth of the model atmosphere (STD), planetary boundary layer (0–2 km, PBL), lower free troposphere (2–5 km, LFT), upper free troposphere (5–10 km, UFT), tropopause-lower stratosphere (10–16 km, TLS) and the middle stratosphere (16–23 km, MST). Initial GOM and HgP concentrations are zero elsewhere. After passage of the thunderstorm, we diagnose the final altitude distribution and deposition of mercury in each simulation.

ACPD
13, 3575–3611, 2013

The second type of experiments conducted examines the atmospheric removal of mercury by convective storms simulated for multiple combinations of CAPE, SHEAR and PW within the defined parameter space (Tables 1, 3). Realistic initial GOM and HgP vertical profiles are used (Fig. 3), as described above. These simulations are conducted starting from initial conditions specified using radiosonde observations from both the Southeast and Northeast sites (Fig. 2). The following naming convention is used to identify the different simulations: cXsYpZ_SID, where X, Y and Z are the values of CAPE, SHEAR and PW, respectively, associated with the radiosonde observation used in the experiment and SID indicates the geographical location. The variable SID can have be "n" or "s" indicating Northeast or Southeast sites. A numerical model simulation, initialized using radiosonde observation from a Southeast site and with a 1000 J kg^{-1} CAPE, 15 m s^{-1} shear and 50 mm PW will be referred to as a c1000s15p50_s experiment. A similar simulation, except initialized using a profile from a Northeast radiosonde site will be referred to as a c1000s15p50_n experiment. Radiosonde observations over both Northeast and Southeast are both utilized in order to account for variability related to environmental parameters in addition to CAPE, SHEAR and PW.

In the second set of experiments, for a given CAPE, response of mercury wet deposition to systematic variations in PW and SHEAR will be examined. For example two simulations where CAPE and PW is held constant, but SHEAR varies will be compared (e.g. c2500s10p50_s v c2500s5p50). An implicit assumption in such comparisons is that majority of the variability is due to the parameter that is altered between the experiments. However, in practice it is difficult to get two atmospheric profiles that have two parameters exactly the same. Other possibility is to artificially modify the atmospheric profile to modify just one characteristic. Since CAPE and PW are interconnected variables it is difficult to change PW without altering CAPE. However, for a given combination of CAPE and PW, differing SHEAR profiles may be imposed by scaling the wind profile. Such shear sensitivity experiment will be conducted by imposing a uniform scaling factor of 0.5 to the wind profile through the depth of the atmosphere.

ACPD
13, 3575–3611, 2013

The sensitivity simulation will be denoted by adding a prefix of _0.5SHEAR to the name of the experiment for which the wind profile is modified by a uniform scale factor. The validity of the assumption implicit in the comparisons of the second set of experiments, will be tested utilizing the SHEAR sensitivity experiments.

The third type of experiments simulates a stratiform precipitation event, to compare the efficacy of mercury removal by stratiform versus convective cloud systems. It is difficult to initiate a stratiform event in an idealized experimental framework used for simulating convective events. For the stratiform simulation, RAMS was initialized using the spatially heterogeneous North American Model (NAM) atmospheric analysis and incorporating realistic atmospheric forcing. A nested grid structure was employed in these experiments to establish an inner domain similar to that used in the idealized simulations for convective events. The RAMS is integrated until a stratiform cloud deck is established and maintained for a time period of two hours, consistent with the life time of the convective events considered in this study.

3 Results

3.1 Frequency of occurrence of radiosonde observations as a function of parameter space

Analysis of radiosonde observations found that, compared to the Northeast sites, the mean CAPE and PW is 62 % and 25 % higher, and SHEAR is 125 % smaller at the Southeast sites (Table 2). Cumulative frequency distributions of CAPE (Fig. 4a) show that ∼65 % of the soundings have CAPE of $\leq 2000\,\mathrm{J\,kg^{-1}}$ at the Northeast sites, whereas it only ∼19 % at the Southeast sites. The highest number of soundings at the Southeast sites falls within the CAPE range $2000\text{–}2500\,\mathrm{J\,kg^{-1}}$ followed by $2500\text{–}3000\,\mathrm{J\,kg^{-1}}$ range. At the Northeast sites, 92 % and 20 % of the radiosonde observations have PW values $<= 50$ mm and SHEAR $<= 8\,\mathrm{m\,s^{-1}}$ respectively (Fig. 4b, c), compared to ∼61 % at 69 % the Southeast sites (Fig. 4b). The contrast between the

ACPD
13, 3575–3611, 2013

sites becomes even more evident when co-occurrences of specific ranges of CAPE, PW and SHEAR are considered (Table 2, Table 3). For example, for moderate PW (50 mm) and all values of CAPE, Southeast sites are most likely to have low SHEAR (s5), while Northeast sites are likely to have higher SHEAR (s10) (Table 3). Of the categories examined here, only the combination of highest SHEAR (15 $\mathrm{m\,s^{-1}}$) and lowest PM (40 mm) occur more frequently in the Northeast than in the Southeast.

Numerical modeling experiments discussed in the following sections will consider thunderstorm development for environments with CAPE of ~2500 $\mathrm{J\,kg^{-1}}$ (highly unstable conditions) which occur frequently over the Southeast (Fig. 4a). Since the unstable conditions also frequently co-occur with smaller values of SHEAR (5 $\mathrm{ms^{-1}}$) over the Southeast sites (Table 3, Fig. 4), numerical modeling experiments are utilized to contrast how mercury concentrations in thunderstorm rainfall is altered in a higher shear environment more prevalent over the Northeast.

3.2 Diagnosis of mercury wet deposition in thunderstorms

We next develop a physical understanding of how thunderstorms transport mercury through a case study of a single storm containing GOM and HgP starting at various altitudes. The c2500s10p60 initial conditions produce a vigorous storm and relatively high wet removal and deposition of atmospheric mercury. This experiment shows that the surface wet deposition is most sensitive to GOM and HgP in the boundary layer (Table 4). Approximately 50 % of mercury mass initially in the PBL is removed through wet deposition. The fraction of mercury deposited to the surface declines with altitude, being 34 % for the lower free troposphere, 11.5 % for the upper tropospheric region and 3.0 % for the tropopause and lower stratosphere and 0.7 % for the middle stratosphere. In the STD simulation with uniform vertical distribution of GOM and HgP, about 60 % of mercury deposited at the surface originates from above 2 km. In reality, the contribution from the upper free troposphere and lower stratosphere (near tropopause) could be larger since GOM and HgP mixing ratios increase with altitude (Fig. 3; Lyman and Jaffe, 2012).

ACPD
13, 3575–3611, 2013

Profiles of domain-averaged perturbation of GOM (Fig. 5a), at the end of the sensitivity experiments LFT and UFT, show an increase in GOM in the boundary layer, caused by both evaporation of precipitation reaching this layer and air mass advection (Fig. 5a). However, in the STD simulation, the gain in GOM in the boundary layer is negated by higher magnitude of loss of GOM from within the layer. Thus, the profile of mean GOM perturbation in the STD experiment is dominated by scavenging except in the region immediately above the PBL (Fig. 5a). In the TLS, UFT and LFT experiments, some HgP is transported downwards (Fig. 5b), but in the STD simulation, HgP removal dominates at all altitudes.

Note that the largest GOM changes in the STD simulation occur at the highest altitudes (Fig. 5a), where little GOM is removed to the surface. This indicates that thunderstorms are mixing the high altitude reservoir of oxidized mercury downwards and making it more susceptible to scavenging by subsequent storms. In areas where thunderstorms occur frequently, this could be a potential pathway for enhanced mercury wet deposition.

3.3 Impact of convective storm morphology on mercury wet deposition and concentration in precipitation

When comparing mercury concentrations in precipitation between different events, confounding effects of differences in amount of precipitation needs to be taken into account. Mercury concentrations in rainfall decrease approximately exponentially with rainfall amount (Holmes et al., 2010b) due to the washout effect, which is also observed for other soluble trace gases and aerosols. Numerical model simulations for parameter combinations c2500s5p50_s, c2500s10p50_s, c2500s5p60_s and c2500s10p60_s also show nearly exponential decrease of mercury in rainfall (Fig. 6a, b), similar to observations.

For a given CAPE (2500 $\mathrm{J\,kg^{-1}}$), the concentration of mercury in rainfall is sensitive to SHEAR, but the nature of the sensitivity depends upon PW. For lower PW conditions (50 mm), increase in SHEAR (5 $\mathrm{m\,s^{-1}}$ to 10 $\mathrm{m\,s^{-1}}$), leads to an increase

ACPD
13, 3575–3611, 2013

in mercury concentrations (Fig. 6a) for lower precipitation amounts (< 13 mm), but a reduction at higher precipitation amounts (> 13 mm). At higher PW conditions (60 mm) increase in SHEAR (Fig. 6b) leads to decrease in mercury concentrations for all the precipitation amounts. To demonstrate that the effect is primarily due to shear, we isolate SHEAR in sensitivity experiments c2500s10p50_s_0.5SHEAR and c2500s10p60_0.5SHEAR, where the shear profiles are uniformly scaled to half the value are utilized (Fig. 6c, d). Differences in mercury concentration in rainfall between c2500s10p50_s and c2500s10p50_s_0.5SHEAR experiments (Fig. 6c) are similar to differences between experiments c2500s5p50_s and c2500s10p50_s experiments. Thus, the differences in mercury concentration between c2500s5p50_s and c2500s10p50_s experiments are caused primarily due to variation in SHEAR. Similarly, differences in mercury concentration between c2500s5p60_s and c2500s10p60_s cases are also explained by the variation of SHEAR (Fig. 6d).

3.4 Vertical distribution of mercury wet deposition removal and mass flux in thunderstorms

Spatial (domain) and temporal average (for the time period of the simulation) of vertical profiles of hydrometeor mixing ratio (both ice and water phase), wet deposition removal of GOM and HgP were computed for the c2500s5p50_s, c2500s10p50_s, c2500s5p60_s and c2500s10p60_s experiments. Note that the spatial average considers only atmospheric columns where hydrometeors are present. For all the cases considered, GOM and HgP scavenging occurs over a deep layer of the atmosphere, extending from the surface to ~ 10 km (Fig. 7). Note that the hail and graupel hydrometeors, which are classified as ice in the figure, carry some liquid water, as well as ice, and thus scavenge GOM at high altitudes where there is no rain. The scavenging of both GOM and HgP in the upper regions of the boundary layer and the lower tropospheric layer increases with PW.

There are substantial differences in mass flux of hydrometeors (transport of mass of hydrometeor per unit area per unit time) and mercury (GOM used as an example)

ACPD
13, 3575–3611, 2013

between c2500s5p50_s, c2500s10p50_s, c2500s5p60_s and c2500s10p60_s experiments (Fig. 8). Both hydrometeor and GOM mass flux increases with PW (Fig. 8a, b). Scavenging of mercury (Fig. 7) and concentrations in rainfall (Fig. 6a, b) are both sensitive to hydrometeor and GOM mass flux in the 0–4 km layer. Note that GOM mass flux in downdrafts have magnitudes similar to those in updrafts, but the cloud mass flux associated with the downdrafts are substantially less (Fig. 8). This is indicative of transport in clear air regions or along the lateral boundary region of the thunderstorm. In all the experiments, there is enhanced GOM flux near the tropopause, despite the small cloud mass flux because the concentration gradients are sharpest at these altitudes (Fig. 3). While such sharp gradients of oxidized mercury have been observed around the tropopause (Lyman and Jaffe, 2012), the large fluxes simulated at these high altitudes have high uncertainty because of the sparse constraints on the gradient in the initial conditions. Above the tropopause, vertical Hg fluxes diminish quickly because the strong stratospheric temperature inversion suppresses cloud vertical motions. This also explains the negligible impact of stratospheric GOM on deposition, seen in the MST simulation above (Sect. 3.2).

3.5 Comparison of mercury concentrations in rainfall in the Northeast and Southeast

Analysis of radiosonde observations (Sect. 3.1) show that differing combinations of CAPE, SHEAR and PW are prevalent over Southeast sites compared to Northeast sites (Fig. 9). Numerical modeling experiments also show that mercury concentration is higher for SHEAR and PW combinations that are more common in the Southeast (Sect. 3.3). However there are other degrees of freedom that need to be considered which could mask or modulate the effects of variability of CAPE, SHEAR and PW. Therefore an ensemble of simulations, involving thunderstorms simulated for parameter combinations that occur frequently over the Northeast and Southeast sites are compared (Fig. 9). The mercury concentration and surface wet deposition for these two different groupings are then plotted as a function of accumulated rainfall (Fig. 9). This

ACPD
13, 3575–3611, 2013

analysis shows that mercury concentrations and wet deposition are generally higher for the Southeast sites, even after accounting for the dilution effect of precipitation amount.

3.6 Mercury concentration in rain: comparison between stratiform and convective events

Uptake of mercury over a deeper layer of the atmosphere is potentially one of the factors that contribute to enhanced mercury wet deposition in thunderstorms in comparison to other types of precipitation systems. Comparison between the stratiform and thunderstorm simulations c2500s5p50_s, c2500s10p50_s, c2500s5p60_s and c2500s10p60_s show higher mercury concentration in the latter, even after accounting for the dilution effect (Fig. 9). In the stratiform experiment, GOM and HgP scavenging only occurs below ∼4.5 km altitude (Fig. 10), whereas in thunderstorms substantial removal occurs up to 10 km (Fig. 7).

4 Discussion

This study shows that meteorological conditions in the Southeast US favor more frequent thunderstorms than in the Northeast and that those conditions favor microphysical and dynamic structures that enhance wet deposition removal of GOM and HgP. Sensitivity studies further show that such thunderstorms are sensitive to both GOM and HgP concentrations in the FT and PBL. Together, these modeling results support the observational finding of Holmes et al. (2010b) that a large part of the Southeast US wet deposition enhancement can be explained by the frequency of thunderstorms and their greater scavenging. These finding suggest that in regions where deep thunderstorms are more frequent, global transport and chemistry of atmospheric mercury is an important factor in determining surface wet deposition of mercury. Thus, thunderstorm scavenging of GOM and HgP from the free troposphere may be one possible explanation for high wet deposition of mercury measured at unpolluted sites such as Puerto

ACPD
13, 3575–3611, 2013

Rico (Shanley et al., 2011) where deep thunderstorm occur frequently in environments with high PW.

It is also important to consider the following constraints associated with the chosen experimental design. First, it was chosen to eliminate confounding factors such as large scale dynamical forcing, chemical transformation etc. Thus this study does not include organized, larger scale convective systems such as mesoscale convective systems. The time scales and circulation patterns associated with such systems are considerably different and their response to changes in environmental conditions such as PW could therefore be substantially different, and the approach taken in this study has to be extended to actual events. Second, in numerical simulations the rainfall mercury concentration can be determined at all grid points within the domain. Observations of wet deposition are often taken at few discrete locations and a large sample size would be required to capture the spatial variability indicated by numerical simulations (Figs. 6 and 9). Oxidation of Hg(0) though photochemistry and aqueous phase reactions are not considered in this study and will be evaluated in future investigations. Cyclic boundary conditions assumed in this study is another limitation since it can reintroduce material removed though the outflow to the inflow. However, since the simulations considered in this study are for short timescales and such effects are expected to be minimal.

5 Conclusions

This study utilized idealized numerical model simulations to examine the budget of mercury within convective clouds and rainfall as a function of environmental characteristics that influence formation and evolution of thunderstorms. Simulations were also conducted to determine the sensitivity of thunderstorms to HgP and GOM concentration in the PBL and FT. The implications of this analysis to enhanced mercury wet deposition along the Gulf Coast are considered. Additional simulation of a stratiform precipitation event was also conducted and processing of mercury by the event is compared against thunderstorms. This comparison is used to understand enhanced

Discussion Paper | Discussion Paper | Discussion Paper | Discussion Paper |

ACPD
13, 3575–3611, 2013

Simulations of mercury scavenging and deposition in thunderstorms

U. S. Nair et al.

mercury concentration in rainfall from thunderstorms. The major conclusions from the study are the following.

1. For conditions of uniform concentration of atmospheric GOM and HgP, about 40 % of mercury deposited from a typical Southeast thunderstorm originates in the boundary layer. The rest of the mercury in rainfall originates above the boundary layer with lower free troposphere layer, upper free troposphere and tropopause-lower stratosphere layers contributing 35 %, 18 % and 6 %, respectively.

2. Mercury concentration in rainfall from thunderstorms is sensitive to SHEAR, but the nature of sensitivity is dependent on PW. At lower values of PW, increase in SHEAR decreases mercury concentration in higher-rain areas and increases concentration in low-rain areas. For higher amounts of PW, increase in SHEAR reduces mercury concentration for all rainfall amounts. Overall, lower SHEAR increases scavenging and deposition of both GOM and HgP. An ensemble of thunderstorm simulations, conducted for parameter combinations that occur frequently over the Northeast and Southeast sites respectively, show that mercury concentration in rainfall is higher under conditions common in the Southeast.

3. Mercury concentration is higher in rainfall from thunderstorms compared to stratiform rainfall. Substantial mercury wet deposition removal occurs up to altitudes of 8km in thunderstorms, where as it is over the lower 4 km for stratiform system considered. Thunderstorms are sensitive to HgP and GOM concentrations in both PBL and the FT. Thus in regions where deep thunderstorms occur frequently, such as the Southeast US and the Gulf Coast, transport of GOM and HgP in the free troposphere may be an important source of deposited mercury.

The sensitivity analysis conducted in this study is an initial attempt to determine whether mercury concentration is enhanced in rainfall from thunderstorms compared to precipitation from other systems such as stratiform clouds. Detailed analysis of physical processes that cause differences in cloud scavenging of mercury is beyond the

ACPD
13, 3575–3611, 2013

scope of this initial work and need to be addressed using modeling of specific events, in conjunction with observational analysis.

Acknowledgements. This research is supported by EPRI.

References

Amos, H. M., Jacob, D. J., Holmes, C. D., Fisher, J. A., Wang, Q., Yantosca, R. M., Corbitt, E. S., Galarneau, E., Rutter, A. P., Gustin, M. S., Steffen, A., Schauer, J. J., Graydon, J. A., Louis, V. L. St., Talbot, R. W., Edgerton, E. S., Zhang, Y., and Sunderland, E. M.: Gas-particle partitioning of atmospheric Hg(II) and its effect on global mercury deposition, Atmos. Chem. Phys., 12, 591–603, doi:10.5194/acp-12-591-2012, 2012.

Barth, M. C., Kim, S.-W., Wang, C., Pickering, K. E., Ott, L. E., Stenchikov, G., Leriche, M., Cautenet, S., Pinty, J.-P., Barthe, Ch., Mari, C., Helsdon, J. H., Farley, R. D., Fridlind, A. M., Ackerman, A. S., Spiridonov, V., and Telenta, B.: Cloud-scale model intercomparison of chemical constituent transport in deep convection, Atmos. Chem. Phys., 7, 4709–4731, doi:10.5194/acp-7-4709-2007, 2007.

Coburn, S., Dix, B., Sinreich, R., and Volkamer, R.: The CU ground MAX-DOAS instrument: characterization of RMS noise limitations and first measurements near Pensacola, FL of BrO, IO, and CHOCHO, Atmos. Meas. Tech., 4, 2421–2439, doi:10.5194/amt-4-2421-2011, 2011.

Cotton, W. R., Alexander, G. D., Hertenstein, R., Walko, R. L., McAnelly, R. L., and Nicholls, M.: Cloud Venting – A review and some new global annual estimates, Earth-Sci. Reviews, 39, 169-206, 1995.

Cotton, W. R., Pielke Sr., R. A., Walko, R. L., Liston, G. E., Tremback, C., Jiang, H., McAnelly, R. L., Harrington, J. Y., Nicholls, M. E., Carrio, G. G., and McFadden, J. P.: RAMS 2001: Current status and future directions. Meteor. Atmos. Phys., 82, 5–29, 2003.

Cohen, C.: A quantitative investigation of entrainment and detrainment in numerically simulated cumulonimbus clouds, J. Atmos. Sci., 57, 1657–1674, 2000.

Cohen, C. and McCaul Jr., E. W.: The sensitivity of simulated convective storms to variations in prescribed single moment microphysics parameters that describe particle distributions, sizes, and numbers, Mon. Weather Rev., 134, 2547–2565, 2006.

ACPD
13, 3575–3611, 2013

Dickerson, R. R., Huffman, G. J., Luke, W. T., Nunnermacker, L. J., Pickering, K. E., Leslie, A. C. D., Lindsey, C. G., Slinn, W. G. N., Kelly, T. J., Daum, P. H., Delany, A. C., Greenberg, J. P., Zimmerman, P. R., Boatman, J. F., Ray, J. D., and Stedman D. H.: Thunderstorms – An important mechanism in the transport of air pollutants, Science, 235, 460–464, 1987.
Dvonch, J. T., Graney, J. R., Marsik, F. J., Keeler, G. J., and Stevens, R. K.: An investigation of source-receptor relationships for mercury in south Florida using event precipitation data, Sci. Total Environ., 213, 95–108, 1998.
Dvonch, J. T., Keeler, G. J., and Marsik, F. J.: The influence of meteorological conditions on the wet deposition of mercury in southern Florida, J. Appl. Meteor., 44, 1421–1435, 2005.
Edgerton, E. S., Hartsell, B. E., and Jansen, J. J.: Mercury speciation in coal-fired power plant plumes observed at three surface sites in the southeastern US, Environ. Sci. Technol., 40, 4563–4570, doi:10.1021/es0515607, 2006.
Environmental Protection Agency, 2011: 2010 Biennial Listing of Fish Advisories, Technical Report EPA-820-F-11-014, available at: http://water.epa.gov/scitech/swguidance/fishshellfish/fishadvisories/upload/technical_factsheet_2010.pdf, last access: 15 November 2011.
Guentzel, J. L., Landing, W. M., Gill, G. A., and Pollman, C. D.: Processes influencing rainfall deposition of mercury in Florida, Environ. Sci. Technol., 35, 863–873, 2001.
Halland, J. J., Fuelberg, H. E., Pickering, K. E., and Luo, M.: Identifying convective transport of carbon monoxide by comparing remotely sensed observations from TES with cloud modeling simulations, Atmos. Chem. Phys., 9, 4279–4294, doi:10.5194/acp-9-4279-2009, 2009.
Holmes, C. D., Jacob, D. J., Corbitt, E. S., Mao, J., Yang, X., Talbot, R., and Slemr, F.: Global atmospheric model for mercury including oxidation by bromine atoms, Atmos. Chem. Phys., 10, 12037–12057, doi:10.5194/acp-10-12037-2010, 2010a.
Holmes, C. D., Jacob, D. J., Samath, N., Landing, W., Fuelberg, H. E., Rudlosky, S. D., Caffrey, J., and Edegeron, E.: Thunderstorms increase mercury concentration in rainfall. Presented at Goldschmidt Conference, Knoxville, Tennessee, USA, 2010b.
Kirkpatrick, C., McCaul Jr., E. W., and Cohen, C.: The motion of simulated convective storms as a function of basic environmental parameters, Mon. Weather Rev., 135, 3033–3051, 2007.
Kirkpatrick, C., McCaul Jr., E. W., and Cohen, C.: Sensitivities of Simulated Convective Storms to Environmental CAPE, Mon. Weather Rev., 139, 3514–3532, 2011.
Knupp, K. R. and Cotton, W. R.: Convective cloud downdraft structure: An interpretive survey, Rev. Geophys., 23, 183–215, 1985.

ACPD
13, 3575–3611, 2013

Landing, W. M., Caffrey, J. M., Nolek, S. D., Gosnell, K. J., and Parker, W. C.: Atmospheric wet deposition of mercury and other trace elements in Pensacola, Florida, Atmos. Chem. Phys., 10, 4867–4877, doi:10.5194/acp-10-4867-2010, 2010.
Levine, S. Z. and Schwartz, S. E.: In-cloud and below-cloud scavenging of nitric acid vapor, Atmos. Environ., 16, 1725–1734, 1982.
Lindberg, S., Bullock, R., Ebinghaus, R., Engstrom, D., Feng, X., Fitzgerald, W., Pirrone, N., Prestbo, E., and Seigneur, C.: A synthesis of progress and uncertainties in attributing the sources of mercury in deposition, Ambio, 36, 19–32, 2007.
Lyman, S. N. and Jaffe, D. A.: Formation and fate of oxidized mercury in the upper troposphere and lower stratosphere, Nat. Geosci., 5, 114–117, doi:10.1038/ngeo1353, 2012.
McCaul Jr., E. W. and Weisman, M. L.: The sensitivity of simulated supercell structure and intensity to variations in the shapes of environmental buoyancy and shear profiles, Mon. Weather Rev., 129, 664–687, 2001.
McCaul Jr., E. W., Cohen, C., and Kirkpatrick, C.: The sensitivity of simulated storm structure, intensity, and precipitation efficiency to the temperature at the lifted condensation level, Mon. Weather Rev., 133, 3015–3037, 2005.
Meyers, M. P., Walko, R. L., Harrington, J. Y., Cotton, W. R.: New RAMS cloud microphysics parameterization. Part II: The two-moment scheme, Atmos. Res., 45, 3–39, 1997.
Nair, U. S., McCaul Jr., E. W., and Welch, R. M.: A climatology of environmental parameters that influence severe storm intensity and morphology. Preprints, 21st Conf. on Severe Local Storms, San Antonio, TX, Amer. Meteor. Soc., 2002.
National Atmospheric Deposition Program: National Atmospheric Deposition Program 2009 Annual Summary, NADP Data Report 2010-01, Illinois State Water Survey, University of Illinois at Urbana-Champaign, IL, 2010.
Northeast Regional Mercury Total Maximum Daily Load: http://www.epa.gov/region1/eco/tmdl/pdfs/ne/tmdl-Hg-approval-doc.pdf (last access: November 2012), 2007.
Shanley, J. B., Engle, M. A., Scholl, M. A., Krabbenhoft, D. P., Brunette, R., and Olson, M. L.: High mercury wet deposition at a “Clean air: site in Puerto Rico, Session TG4B-P17, Atmospheric Mercury: Measurement and Monitoring, The 10th International Conference on Mercury as Global Pollutant, 24–29 July 2011, Halifax, Nova Scotia, Canada, 2011.
Seinfeld, J. H. and Pandis, S. N.: Atmospheric Chemistry and Physics: From Air Pollution to Climate Change, 2nd Edition, J. Wiley, New York, 2006.

ACPD
13, 3575–3611, 2013

Simulations of mercury scavenging and deposition in thunderstorms

U. S. Nair et al.

Selin, N. E. and Jacob, D. J.: Seasonal and spatial patterns of mercury wet deposition in the United States: Constraints on the contribution from North American anthropogenic sources, Atmos. Environ., 42, 5193–5204, doi:10.1016/j.atmosenv.2008.02.069, 2008.

Sigler, J. M., Mao, H., and Talbot, R.: Gaseous elemental and reactive mercury in Southern New Hampshire, Atmos. Chem. Phys., 9, 1929–1942, doi:10.5194/acp-9-1929-2009, 2009.

Sillman, S., Marsik, F. J., Al-Wali, K. I., Keeler, G. J., and Landis, M. S.: Reactive mercury in the troposphere: Model formation and results for Florida, the northeastern United States, and the Atlantic Ocean, J. Geophys. Res.-Atmos., 112, D23305, doi:10.1029/2006JD008227, 2007.

Talbot, R., Mao, H., Scheuer, E., Dibb, J., and Avery, M.: Total depletion of Hg^0 in the upper troposphere-lower stratosphere, Geophys. Res. Lett., 34, L23804, doi:10.1029/2007GL031366, 2007.

Valente, R. J., Shea, C., Humes, K. L., and Tanner, R. L.: Atmospheric mercury in the Great Smoky Mountains compared to regional and global levels, Atmos. Environ., 41, 1861–1873, doi:10.1016/j.atmosenv.2006.10.054, 2007.

Voudouri, A. and Kallos, G.: Validation of the integrated RAMS-Hg modeling system using wet deposition observations for eastern North America, Atmos. Environ., 41, 5732–5745, 2007.

Walko, R. L., Cotton, W. R., Meyers, M. P., and Harrington, J. Y.: New RAMS cloud microphysics parameterization. Part I: the single-moment scheme. Atmos. Res., 38, 29–62, 1995.

White, E. M., Keeler, G. J. and Landis, M. S.: Spatial variability of mercury wet deposition in Eastern Ohio: Summertime meteorological case study analysis of local source influences, Environ. Sci. Technol., 43, 4946–4955, 2009.

Yin, Y., Parker, D. J., and Carslaw, K. S.: Simulation of trace gas redistribution by convective clouds – Liquid phase processes, Atmos. Chem. Phys., 1, 19–36, doi:10.5194/acp-1-19-2001, 2001.

ACPD
13, 3575–3611, 2013

Simulations of mercury scavenging and deposition in thunderstorms

U. S. Nair et al.

ACPD
13, 3575–3611, 2013

Simulations of mercury scavenging and deposition in thunderstorms

U. S. Nair et al.

Table 1. The name and discrete value ranges of CAPE, SHEAR and PW considered in this study.

Variable	CAPE (J kg^{-1})				SHEAR (m s^{-1})			PW (mm)		
Category Name	c1000	C1500	c2000	c2500	s5	s10	s15	p40	p50	p60
Mean Value Range	1000 ± 100	1500 ± 100	2000 ± 100	2500 ± 100	5 ± 2	10 ± 2	15 ± 2	40 ± 2	50 ± 2	60 ± 2

Table 2. Average and standard deviation of CAPE, SHEAR, and PW over the Eastern United States during 2001–2011. See Fig. 2 for radiosonde sites used in the analysis.

Location (profiles)	CAPE (J kg^{-1})	SHEAR (m s^{-1})	PW (mm)
South ($n = 4631$)	1324.0 ± 896.5	6.1 ± 3.6	46.8 ± 9.2
North ($n = 3770$)	813.9 ± 1046.7	13.6 ± 5.3	37.4 ± 8.6

ACPD
13, 3575–3611, 2013

Table 3. Co-occurrence of specific value ranges of CAPE (c1000, c1500, c2000 and c2500), SHEAR (s5 and s10) and PW (p40 and p50) at the southern and northern sites for summer months of 2000–2011. The counts for the northern sites are given in parenthesis.

	p50	**p60**
s5	**c1000** – 73 (2) **c1500** – 36 (0) **c2000** – 36 (0) **c2500** – 13 (0) 158 (2)	**c1000** – 11 (0) **c1500** – 21 (1) **c2000** – 9 (0) **c2500** – 14 (0) 55 (1)
s10	**c1000** – 29 (12) **c1500** – 19 (4) **c2000** – 20 (2) **c2500** – 9 (3) 77 (21)	**c1000** – 4 (2) **c1500** – 6 (0) **c2000** – 3 (0) **c2500** – 4 (1) 17 (3)

ACPD
13, 3575–3611, 2013

Simulations of mercury scavenging and deposition in thunderstorms

U. S. Nair et al.

Table 4. Fraction of mercury mass (%) transported from an initial altitude to a final altitude by the passage of a thunderstorm. Transport includes advection and within precipitation. Each column corresponds to an experiment initialized with 30 pg m^{-3} GOM and HgP in the specified initial altitude range and zero elsewhere. The STD experiment has uniform 30 pg m^{-3} initial mixing ratios through the entire column. The total mass of mercury in each experiment is 71.3 ng m^{-2} (PBL), 98.5 ng m^{-2} (LFT), 148 ng m^{-2} (UFT), 162 ng m^{-2} (TLS), 180.9 ng m^{-2} (MST), and 661 ng m^{-2} (STD).

	Initial Altitude					
Final Altitude	PBL (0–2 km)	LFT (2–5 km)	UFT (5–10 km)	TLS (10–16 km)	MST (16–23 km)	STD (0–23 km)
16–23 km	0.0	0.0	0.0	5.7	96.2	26.9
10–16 km	0.0	0.0	1.5	88.4	3.1	25.3
5–10 km	0.0	0.7	83.4	2.6	0.0	18.7
2–5 km	1.3	62.8	3.3	0.3	0.0	10.1
0–2 km	47.2	2.2	0.3	0.0	0.0	5.3
Surface deposition and	51.5	34.4	11.5	3.0	0.7	13.7
(deposited mass, pg m^{-3})	(36.7)	(33.6)	(17.0)	(5.6)	(1.3)	(94.7)

ACPD
13, 3575–3611, 2013

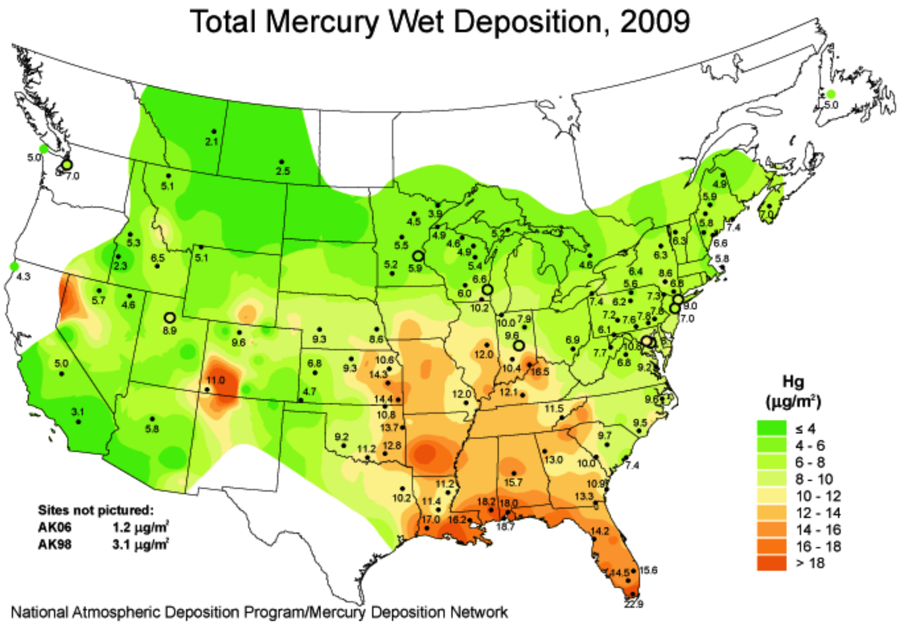

Fig. 1. Total mercury wet deposition for the year 2009. Note the regional maximum along the Gulf Coast. This is a consistent feature that is also present during other years (National Atmospheric Deposition Program, 2010).

ACPD
13, 3575–3611, 2013

Simulations of mercury scavenging and deposition in thunderstorms

U. S. Nair et al.

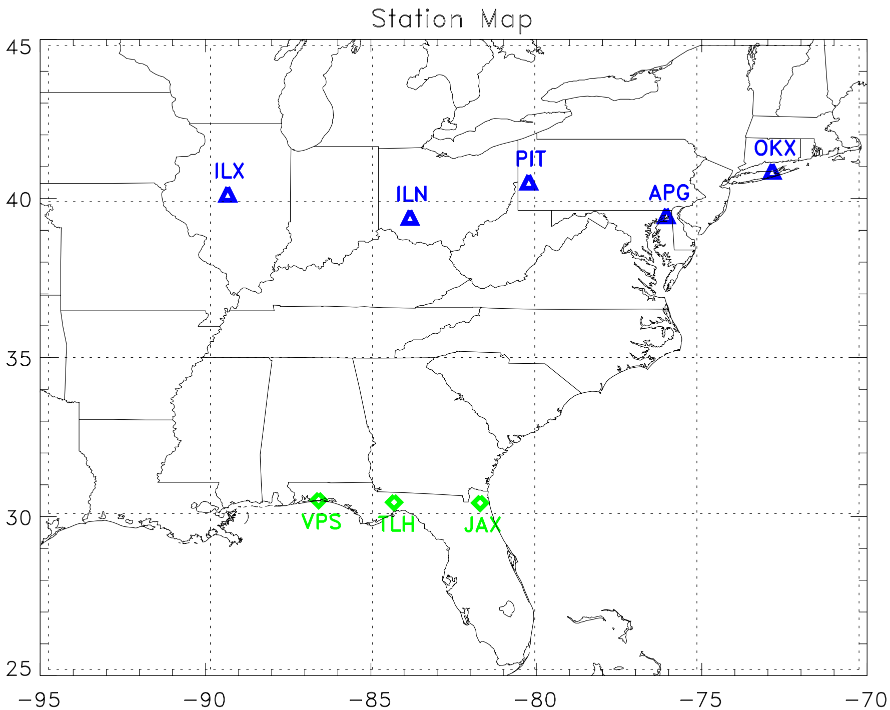

Fig. 2. Launch sites for the radiosondes used in the present study. Blue triangles denote the northern stations located at around 40° N, green diamonds denote the southern stations near 30° N.

ACPD
13, 3575–3611, 2013

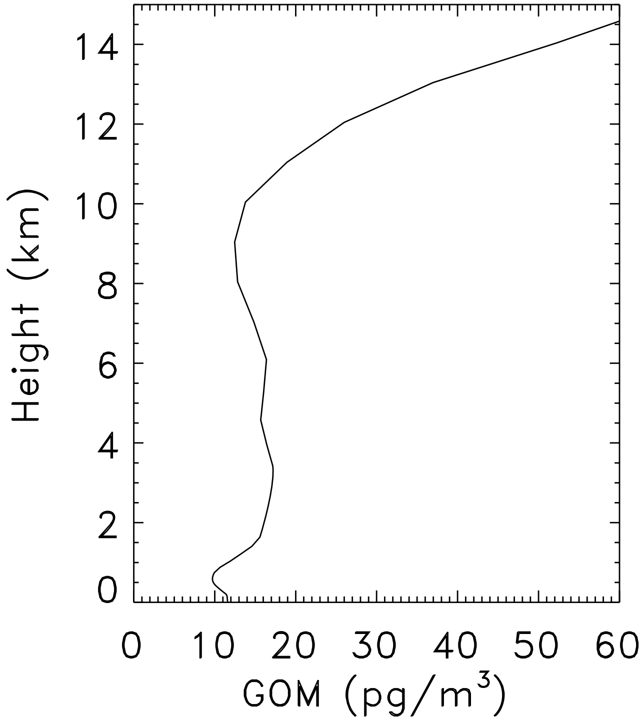

Fig. 3. Initial GOM profile for the southern sites derived from GEOS-Chem simulations. The profiles for HgP is same as the GOM profile.

ACPD
13, 3575–3611, 2013

Simulations of mercury scavenging and deposition in thunderstorms

U. S. Nair et al.

Title Page
Abstract Introduction
Conclusions References
Tables Figures
◀◀ ▶▶
◀ ▶
Back Close
Full Screen / Esc
Printer-friendly Version
Interactive Discussion

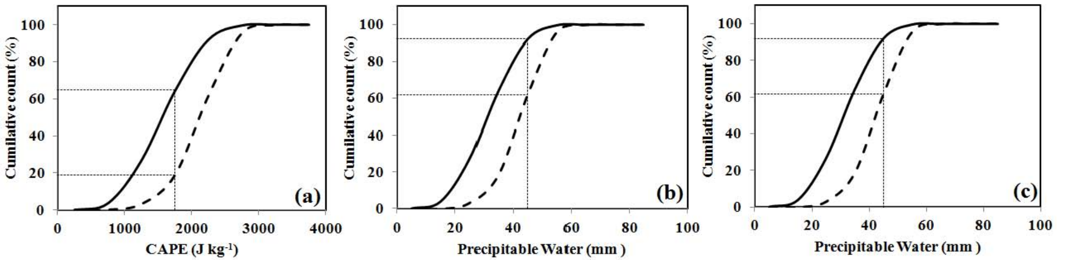

Fig. 4. Cumulative frequency distribution of **(a)** CAPE; **(b)** PW and; **(c)** SHEAR for the time period 2000–2011. The thick solid line is for the northern sites and the thick dashed line is for the southern sites.

ACPD
13, 3575–3611, 2013

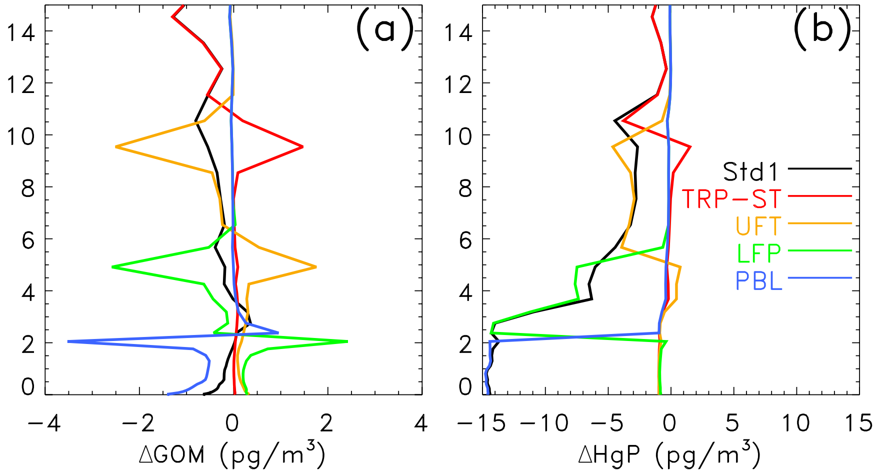

Fig. 5. Domain averaged perturbation of GOM **(a)** and HgP **(b)** at the end of the following simulations: PBL (blue), LFP (green), UFT (orange), TLS (red) and STD (black) sensitivity experiments.

ACPD
13, 3575–3611, 2013

Simulations of mercury scavenging and deposition in thunderstorms

U. S. Nair et al.

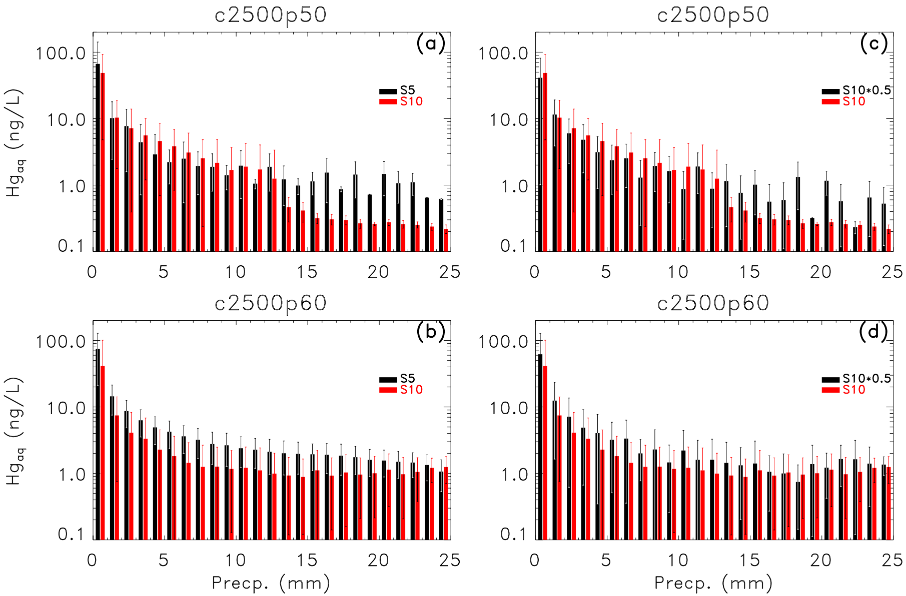

Fig. 6. Mercury concentration as a function of accumulated rainfall for **(a)** and **(c)**, CAPE in c2500 and PW in p50; **(b)** and **(d)**, CAPE in c2500 and PW in p60. For **(a)** and **(b)** SHEAR categories s5 (black) and s10 (red). For **(c)** and **(d)** SHEAR categories s10 (red) and divided by 2 (black).

ACPD
13, 3575–3611, 2013

Simulations of mercury scavenging and deposition in thunderstorms

U. S. Nair et al.

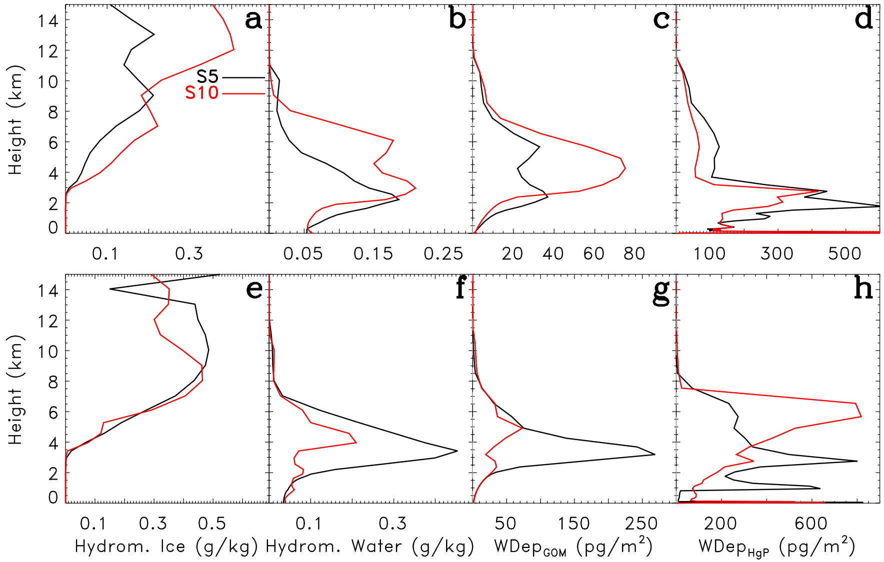

Fig. 7. Vertical average profiles of hydrometeors and scavenging in thunderstorms. **(a)** Frozen hydrometeors; **(b)** rain (liquid hydrometeors); **(c)** net scavenging of GOM; **(d)** net scavenging of HgP. Category s5 is in black and s10 in red. CAPE is in c2500 for all simulations. Panels **(a–d)** are PW category p50. Panels **(e–h)** are PW category p60. Note the change of scale between the top and bottom rows.

ACPD
13, 3575–3611, 2013

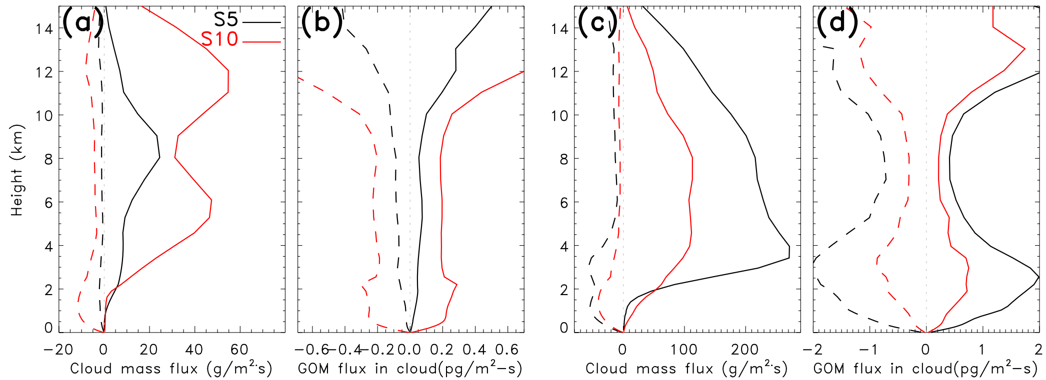

Fig. 8. Cloud mass flux and GOM flux in clouds for SHEAR categories 5 ms^{-1} (black) and 10 ms^{-1} (red). Panel **(a)** is average could mass flux and **(b)** is GOM mass flux in cloud for CAPE category c2500 and PW in p50. Panels **(c)** and **(d)** are the same as **(a)** and **(b)**, except for CAPE in c2500 and PW in p60. Solid lines show updrafts while downdrafts are dashed.

ACPD
13, 3575–3611, 2013

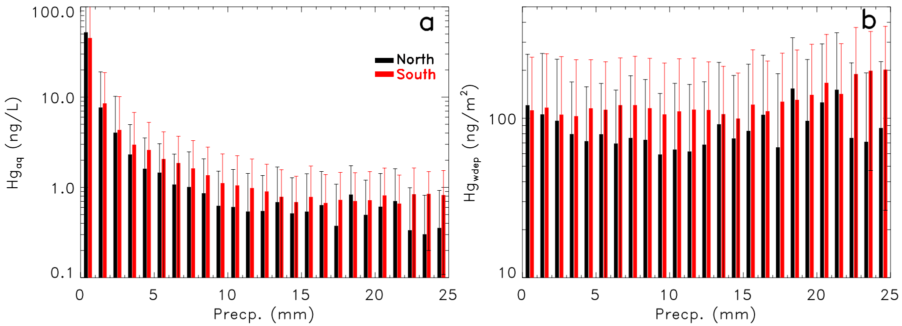

Fig. 9. Mercury concentration **(a)** and wet deposition **(b)** as a function of accumulated rainfall. The red and black bars show simulations initialized with radiosonde profiles from northern sites and southern sites, respectively. The northern simulations comprise 7 cases from categories of low CAPE and PW and higher SHEAR (c1000-1500, s10, and p30–40); the southern simulations comprise 18 cases from 12 highest occurrence categories that have moderate to high CAPE and PW and lower SHEAR.

ACPD
13, 3575–3611, 2013

Simulations of mercury scavenging and deposition in thunderstorms

U. S. Nair et al.

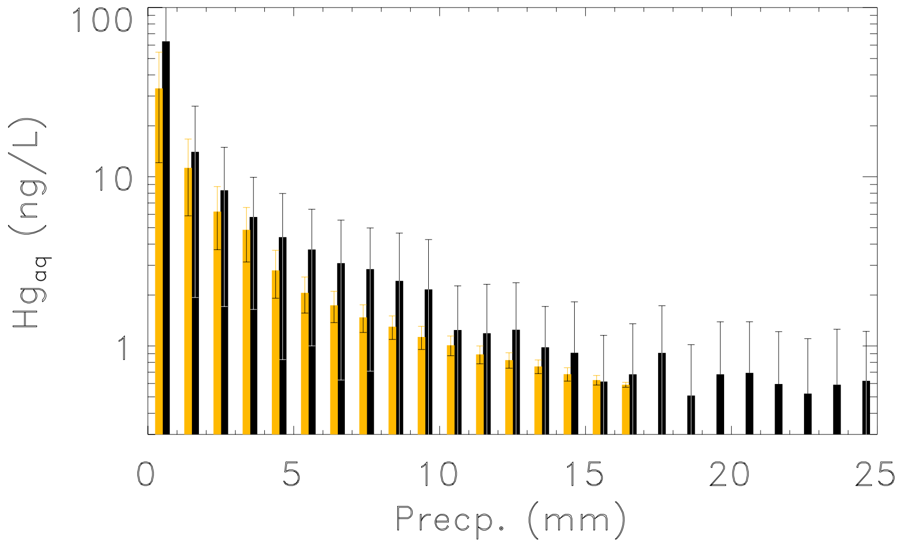

Fig. 10. Mercury concentration in rainfall from a stratiform event (yellow) and thunderstorms simulations c2500s5p50_s, c2500s10p50_s, c2500s5p60_s and c2500s10p60_s (black). All simulations are initialized with identical GOM and HgP conditions.

ACPD
13, 3575–3611, 2013

Simulations of mercury scavenging and deposition in thunderstorms

U. S. Nair et al.

Title Page
Abstract | Introduction
Conclusions | References
Tables | Figures
◀| |▶
◀ ▶
Back | Close
Full Screen / Esc
Printer-friendly Version
Interactive Discussion

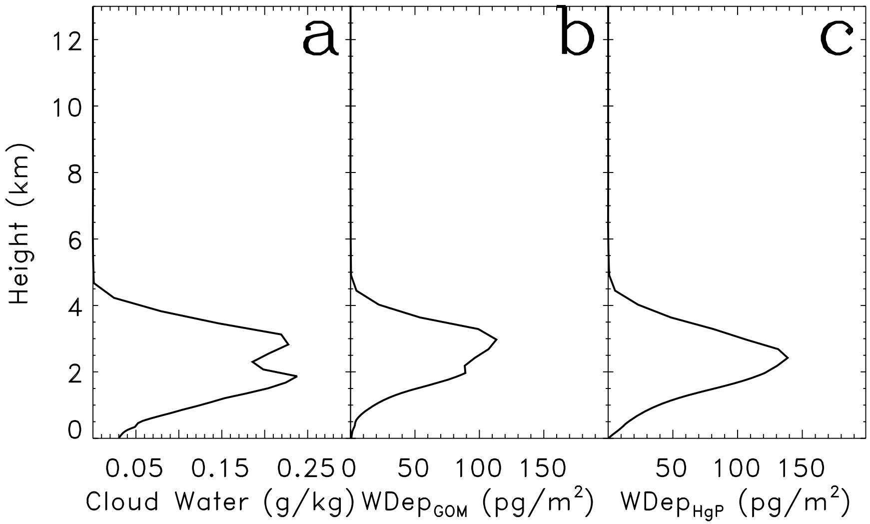

Fig. 11. Domain averaged vertical distribution of: **(a)** hydrometeor in water phase; **(b)** GOM wet deposition; **(c)** HgP wet deposition for the stratiform event.

ACPD
13, 3575–3611, 2013